## Title
Effect of Relative Density on the Drained Seismic Compression of Unsaturated Backfills



ISBN
978-3-030-77237-6

Authors
Rong, Wenyong
McCartney, John S

Publication Date
2022

DOI
10.1007/978-3-030-77238-3_21

Peer reviewed

# Effect of Relative Density on the Drained Seismic Compression of Unsaturated Backfills

Wenyong Rong[1], S.M.ASCE, John S. McCartney[2], Ph.D., P.E., F.ASCE

[1] Graduate Research Assistant, Department of Structural Engineering, University of California, San Diego, La Jolla, CA 92093-0085; Email: w1rong@eng.ucsd.edu
[2] Professor and Department Chair, Department of Structural Engineering, University of California, San Diego, La Jolla, CA 92093-0085; Email: mccartney@ucsd.edu

**Abstract.** It is critical to accurately predict the seismic compression of backfill soils supporting bridge decks, pavements, or railways as small backfill settlements may have substantial impacts on the performance of these overlying transportation systems. Although several studies have evaluated the seismic compression of loose unsaturated soils, there has not been significant focus on the seismic compression of denser soils. This study presents the results from series of strain-controlled cyclic simple shear tests performed on unsaturated sand specimens having different initial relative densities and initial matric suctions representative of near-surface backfills. Although the seismic loading process may involve rapid, undrained shearing, the cyclic simple shear tests were performed in drained conditions with a slow shearing rate to isolate the effect of matric suction. The results showed that soils with higher initial suctions (or lower initial degrees of saturation) experienced smaller volumetric strains, but the effect of suction (or degree of saturation) decreases as the relative density increases.

**Keywords:** Seismic Compression, Unsaturated Backfills, Matric Suction, Relative Density

## 1 Introduction

Seismic compression is defined as the accrual of contractive volumetric strains in soils during earthquake shaking and has been recognized as a major cause of seismically induced damage to civil infrastructure (Stewart et al. 2001), i.e. transportation systems. The state-of-the-practice method used to predict contractive volumetric strains of soils during earthquake involves use of a chart developed by Tokimatsu and Seed (1987) correlating volumetric strain with cyclic stress ratio and corrected standard penetration blow count. This chart was developed based solely on results from cyclic simple shear tests on saturated and dry quartz sands from Silver and Seed (1971). However, natural soil layers near the ground surface are often above the water table and may be unsaturated, especially for the compacted backfill soil layers in engineered transportation systems, i.e. roadways, retaining walls and slopes, bridge abutment, etc., which are designed with the intention of remaining in unsaturated conditions by provision of adequate drainage. In earthquake-prone areas, it is of great significance to predict the potential maximum seismically-induced settlements of backfills as small settlements may have a significant effect on the normal operation of these transportation systems.

The behavior of unsaturated backfill soils during earthquake shaking is uncertain. At one extreme, liquefaction without volume change is expected in fully saturated soils, while at the other extreme, volumetric contraction is expected in dry soils. Several experimental studies have characterized the seismic compression of unsaturated sand at various relative densities under undrained shearing or without consideration of drainage conditions (Hsu and Vucetic 2004; Whang et al. 2004; Duku et al. 2008; Unno et al. 2008; Okamura and Soga 2006; Kimoto et. 2011; Ghayoomi et al. 2011; Rong and McCartney 2020). While some of these studies did not observe a clear trend in the volumetric strain with matric suction (or degree of saturation) for a limited number of cyclic shear strain amplitudes (e.g., Hsu and Vucetic 2004; Whang et al. 2004; Duku et al. 2008), they did not control unsaturated conditions or measure changes in degree of saturation or matric suction during shearing. The lack of a clear trend may also be due to the wet tamping method used to reach different initial suctions, which might result in large uncertainties in soil structures. Although denser soils showed higher resistance to seismic compression at the same unsaturated state (Whang et al. 2004; Duku et al. 2008), the controlling or the dominant factor affecting seismic compression of unsaturated soils has not been discussed. Unno et al. (2008) and Kimoto et al. (2011) performed undrained and drained cyclic triaxial tests on unsaturated soils with various levels of suction and observed volumetric contraction of dense and loose sands along with the buildup of both the pore water pressure and the pore air pressure. They observed a clear effect of the degree of saturation with liquefaction occurring in some tests on sands at higher degrees of saturation and a clear effect of relative density with denser state resulting in smaller seismic compressions. However, only two initial suctions and relative density values were evaluated, and they did not separate the effects of relative density and degree of saturation on the seismic compression as well. Le and Ghayoomi (2017) observed lower seismic compressions for unsaturated specimens with higher suctions in drained cyclic simple shear test. Rong and McCartney (2020) performed drained cyclic simple shear tests (constant suction) on unsaturated sands in the funicular regime and the seismic compression was observed to have a log-linear relation with matric suction, but only the relative density of 0.45 was evaluated in these studies and the effect of relative density remains unknown. Therefore, further experimental study on seismic compression of unsaturated specimens with various initial suctions and various relative densities is needed to help understand the governing mechanisms.

To evaluate the effect of relative density on the seismic compression of unsaturated soils, a series of cyclic simple shear tests on unsaturated specimens with four different initial suctions at each of the three relative densities were performed in this study, representing the general compaction states of near-surface backfills in transportation systems. Although the seismic loading process may involve rapid, undrained shearing, the cyclic simple shear tests were performed in drained conditions with a slow shearing rate to provide a worst-case scenario on the measured seismic compression.

## 2 Effective Stress for Unsaturated Soils

Many mechanical properties of soils, i.e. the shear strength, shear modulus, and damping ratio, are fundamentally influenced by the effective stress. To extend the mechanistic framework established for saturated soils to unsaturated soils, Bishop (1959) proposed the following effective stress for unsaturated soils:

$$\sigma' = (\sigma - u_a) + \chi(u_a - u_w) \quad (1)$$

where σ is the total normal stress on a given plane, $u_a$ is the pore air pressure, $u_w$ is the pore water pressure, the difference between the total normal stress and the pore air pressure represents the net normal stress, the difference between the pore air pressure and the pore water pressure is the matric suction (also denotes as ψ), and χ is Bishop's effective stress parameter. Many definitions of the effective stress parameter χ have been proposed in the literature, some related to the suction and others related to the degree of saturation. Lu et al. (2010) proposed a term called the suction stress $\sigma^s$ that incorporated all interparticle forces and assumed χ is equal to the effective saturation $S_e$ so that the soil water retention curve (SWRC), which quantifies the relation between suction and the degree of saturation within soils, can be integrated into the definition of effective stress. Specifically, the effective saturation can be related to the suction through the van Genuchten (1980) SWRC model, given as follows:

$$S_e = \left\{\frac{1}{1 + [\alpha_{vG}\ (u_a - u_w)]^{N_{vG}}}\right\}^{1-\frac{1}{N_{vG}}} \quad (2)$$

where $\alpha_{vg}$ and $N_{vg}$ are the van Genuchten (1980) SWRC fitting parameters. The effective stress definition of Lu et al. (2010) obtained by combining Equations (1) and (2) is given as follows:

$$\sigma' = (\sigma - u_a) + \left[\frac{u_a - u_w}{\left(1 + \left[\alpha_{vg}(u_a - u_w)\right]^{N_{vg}}\right)^{1-\frac{1}{N_{vg}}}}\right] \quad (3)$$

In this equation, the term in brackets can be referred to as the suction stress $\sigma^s$, and the relationship between suction stress and matric suction (or degree of saturation) is referred to as the suction stress characteristic curve (SSCC). In this study, Equation (3) will be used to quantify the effective stress state of unsaturated soils.

## 3 Sand Properties

The sand used in this study is classified as a well-graded sand (SW) according to the Unified Soil Classification System (USCS). The particle size distribution curve of the well-graded sand is shown in Figure 1. The mean grain size $D_{50}$ and the effective grain size $D_{10}$ are 0.8 mm and 0.2 mm, respectively. The sand has a coefficient of uniformity of $C_u$ = 6.1 and a coefficient of curvature of $C_c$ = 1.0. The specific gravity is 2.61, and the maximum and minimum void ratios are 0.853 and 0.371, respectively.

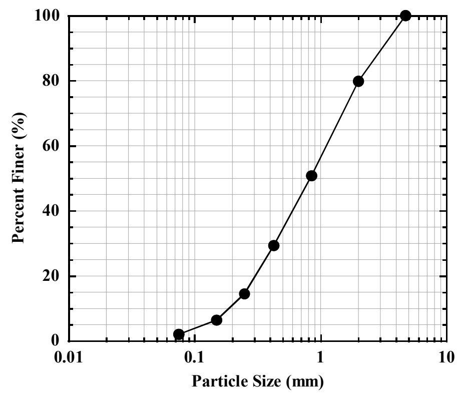


**Figure 1.** Particle size distribution curve of the well-graded sand

**Table 1.** Summary of the basic mechanical of the well-graded sand

| Parameter | Value |
|---|---|
| Specific gravity, $G_s$ | 2.61 |
| Effective grain size, $D_{10}$ (mm) | 0.20 |
| Mean grain size, $D_{50}$ (mm) | 0.80 |
| Coefficient of curvature, $C_c$ | 1.00 |
| Coefficient of uniformity, $C_u$ | 6.10 |
| Maximum void ratio, $e_{max}$ | 0.853 |
| Minimum void ratio, $e_{min}$ | 0.371 |

The SWRC of the well-graded sand at different relative densities were measured using a hanging column that can apply higher suction magnitudes to the residual saturation of the sand. To determine the SWRC, a pre-determined mass of dry sand was poured at a constant rate from a funnel into a Buchner funnel having a fritted glass disk with an air-entry suction of 50 kPa at the bottom that was filled with de-aired water. It was found that a target density of 0.45 could be reached reliably without tamping, however, to reach higher initial relative densities, i.e. $D_r$ = 0.70 and 0.85, different tamping efforts were needed. This initially saturated specimen was incrementally desaturated by applying negative water pressures ($u_w$) to the hanging column while leaving the surface of the specimen open to the atmosphere (which means pore air pressure $u_a$ = 0). Once the outflow of water from the bottom boundary remained constant over a time between readings of 30 minutes, the sand specimen was considered to be at hydraulic equilibrium. Test results including the primary drying path for different relative densities are shown in Figure 2, which also shows the fitted van Genuchten (1980) SWRCs. The best-fit SWRC model parameters for the well-graded sand at different relative densities are summarized in Table 2.

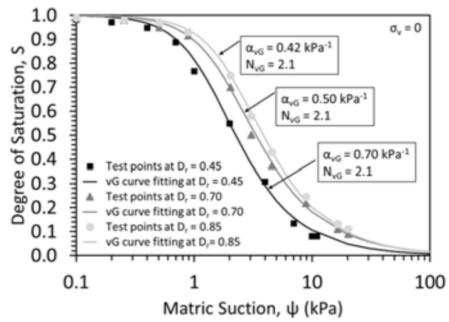


**Figure 2.** SWRCs of the well graded sand at different relative densities

**Table 2.** The van Genuchten fitting parameters of the sand at different relative densities

| Relative density, $D_r$ | $\alpha_{vG}$ ($kPa^{-1}$) | $N_{vG}$ | Saturated volumetric water content, $\theta_s$ | Residual volumetric water content, $\theta_r$ |
|---|---|---|---|---|
| 0.45 | 0.70 | 2.10 | 0.39 | 0 |
| 0.70 | 0.50 | 2.10 | 0.33 | 0 |
| 0.85 | 0.42 | 2.10 | 0.31 | 0 |

The best-fit values of the parameters $a_{vG}$ and $N_{vG}$ for the drying path were used to define the SSCCs at different relative densities, which were plotted in terms of both matric suction and degree of saturation in Figure 3(a) and 3(b), respectively. As $N_{vG}$ is slightly larger than 2.0 at all three relative densities, the SSCCs will not increase monotonically with suction (Lu et al. 2010). Instead, the SSCCs increase with suction (or decreasing degree of saturation) up to the maximum values at intermediate matric suctions before decreasing back to zero at higher suctions.

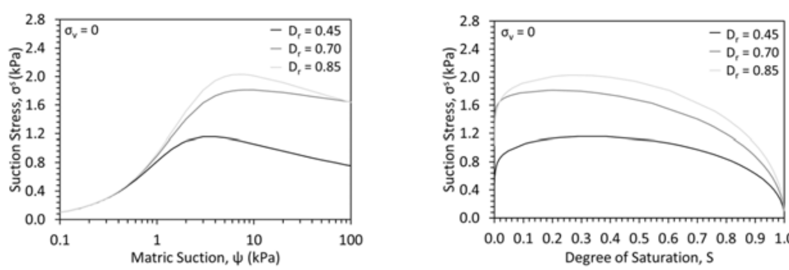


(a) $\sigma^s$ vs ψ (b) $\sigma^s$ vs S

**Figure 3.** SSCCs of the well graded sand at different relative densities

## 4 Simple Shear Device with Suction-Saturation Control

Cyclic simple shear tests allow the principal stress axes to rotate smoothly during cyclic shearing and permit simulation of the stress-strain response of soils in a free-field soil layer due to upward horizontal seismic shear wave propagation, while permitting evaluation of the associated changes in pore water pressure and/or volume change. A monotonic simple shear apparatus manufactured by the Norwegian Geotechnical Institute (NGI) was modified to perform cyclic simple shear tests over a range of shear strain amplitudes and unsaturated conditions (different matric suctions or degrees of saturation) by incorporating a hanging column setup, details of the modification can be found in Rong and McCartney (2020). The overall view of the simple shear apparatus including different components is shown in Figure 4.

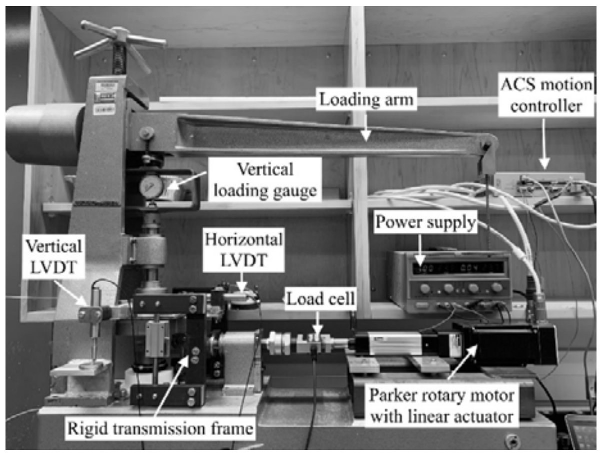


**Figure 4.** Cyclic simple shear apparatus for unsaturated soils

The specimen housing designed to test unsaturated soils in the modified cyclic simple shear device is shown in Figure 5. The top platen incorporates a coarse porous stone which facilitates air drainage while providing a rough surface to transmit shear stresses to the top of the specimen. The bottom platen incorporates a high air-entry porous disk that transmits water from a hanging column consistent with ASTM D6836, which has a central port to accommodate a tensiometer (model T5 from UMS) to monitor changes in matric suction during cyclic shearing. The cylindrical specimen has a height of 20 mm and a diameter of 66.7 mm, resulting in a height to diameter ratio of H/D = 0.3, which is less than the maximum value of 0.4 set by ASTM D6528 (ASTM 2017). The specimen is confined within a wire-reinforced rubber membrane manufactured by Geonor, which minimizes radial deformations of the specimen during preparation, application of vertical stresses, and cyclic shearing but allows vertical and shear deformations.

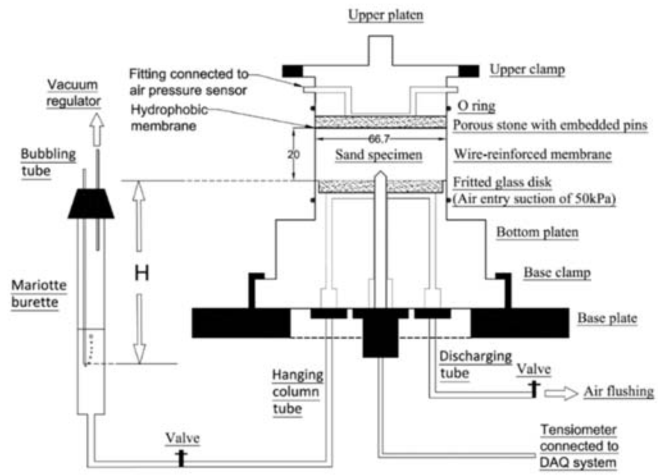


**Figure 5.** Schematic view of the specimen housing used in the NGI-type apparatus

## 5 Preparation of Unsaturated Specimens with Different Relative Densities

The bottom platen of the specimen housing was first fastened on the simple shear device using the T-clamps, and T5 tensiometer was inserted through the porous glass disk and sealed into place. To prepare unsaturated test specimens with different relative densities and different initial suctions, saturated specimens at different relative densities were first prepared and suction was applied subsequently to reach different initial suctions. Like approaches adopted in measuring the SWRCs, pre-determined mass of dry sand was poured from a funnel into the chamber surrounded by the wire-reinforced rubber membrane that was filled with de-aired water to form the uniformly distributed saturated specimen. The target relative density of 0.45 could be reached reliably without tamping, but to reach higher relative densities of 0.70 and 0.85, the specimen was carefully compacted with different amount of energy at three layers. Saturated specimens at different relative densities were then desaturated to different target matric suctions using the hanging column. Water outflow was monitored while monitoring the tensiometer reading to confirm the initial unsaturated states. Once the reading of the tensiometer was constant and the water outflow did not change over an interval of 30 minutes, the unsaturated specimen is assumed to be at hydraulic equilibrium.

## 6 Testing Procedure and Testing Program

Unsaturated specimens with four initial suction values at the three relative densities, marked A, B, C, D in Figure 6(a), were evaluated in this study so that effect of relative density on the seismic compression of unsaturated backfills in drained conditions can be analyzed. As the cyclic shearing was performed in drained conditions, the valve on the hanging column burette was kept open and suction was maintained constant while monitoring any outflow of water. Constant shear strain amplitude of 5% was applied with the same number of cycles N = 200 for all tests in this study, which aims to apply sufficiently large values to result in measurable seismic compressions, shown in Figure 6(b). A shear strain rate of 0.833%/min was chosen to ensure drainage for both the pore water and the pore air based on the matric suction measurement in preliminary testing, which led to a period of 6 minutes. A vertical stress of 50 kPa was applied to the top of the specimen in all tests, which is representative of a near-surface unsaturated backfill soil layer in transportation systems. Before starting the cyclic shearing test, the actual height of the specimen under the applied vertical stress was measured so that the volumetric strain during cyclic shearing can be calculated. The initial states of the unsaturated specimens, like the initial specimen height $h_0$, initial matrix suction $\psi_0$, initial degree of saturation $S_0$, initial gravimetric water content $w_0$, initial volumetric water content $\theta_{w0}$, are presented in Table 3.

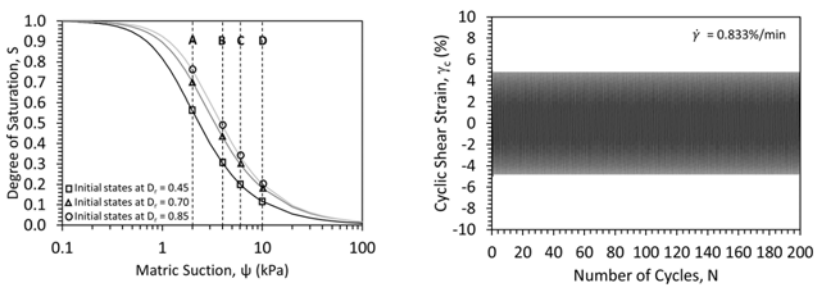


(a) Initial states on SWRCs (b) Applied cyclic shear strains

**Figure 6.** Initial unsaturated conditions and the applied shear strains in the test

**Table 3.** Initial states of the unsaturated specimens

| $D_r$ | SPECIMEN | $h_0$ (mm) | $\psi_0$ (kPa) | $S_0$ | $w_0$ | $\theta_{w0}$ |
|---|---|---|---|---|---|---|
| 0.45 | A-45 | 20.03 | 2.05 | 0.55 | 0.135 | 0.214 |
| | B-45 | 19.98 | 3.98 | 0.31 | 0.075 | 0.119 |
| | C-45 | 19.85 | 5.94 | 0.20 | 0.050 | 0.079 |
| | D-45 | 20.04 | 10.08 | 0.12 | 0.028 | 0.045 |
| 0.70 | A-70 | 20.06 | 1.98 | 0.70 | 0.134 | 0.233 |
| | B-70 | 19.85 | 3.95 | 0.42 | 0.081 | 0.141 |
| | C-70 | 19.95 | 6.02 | 0.28 | 0.054 | 0.094 |
| | D-70 | 19.94 | 10.10 | 0.17 | 0.032 | 0.055 |
| 0.85 | A-85 | 19.89 | 2.05 | 0.75 | 0.129 | 0.233 |
| | B-85 | 19.84 | 3.92 | 0.49 | 0.085 | 0.153 |
| | C-85 | 19.97 | 6.02 | 0.34 | 0.058 | 0.104 |
| | D-85 | 20.02 | 9.98 | 0.20 | 0.035 | 0.063 |

# 7 Experimental Results and Discussion

An example of the time histories of the measured variables in the test are shown in Figure 7 for the unsaturated specimen having an initial suction of 10 kPa at the relative density of 0.70, during the application of 200 cycles of the shear strain amplitude of 5%. Volumetric contraction was observed, and it was found to gradually increase with number of cycles but with a decreased rate, shown in Figure 7(a). As volumetric contraction occurs, the shear stress required to maintain the same shear strain amplitude gradually increases with cycles of shearing, shown in Figure 7(b). Pore water pressure was measured directly with the T5 tensiometer at the bottom of the specimen, shown in Figure 7(c). It was found to increase a little bit at the beginning of shearing but stabilized to the negative value of the initial suction in the subsequent loading cycles due to dissipation or redistribution of the pore water pressure. Water was observed to outflow primarily in the first 100 cycles (the first 600 minutes) and became stabilized subsequently, shown in Figure 7(c) as well. The hysteretic stress strain relationship is shown in Figure 7(d).

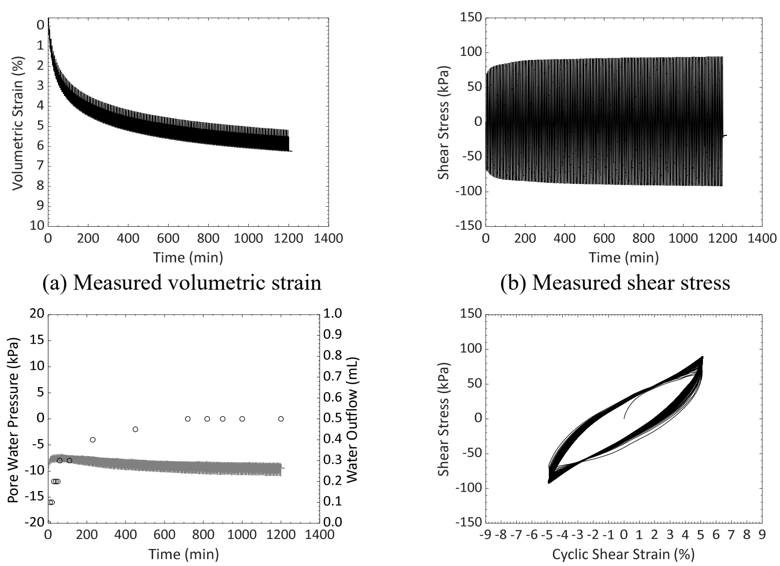


(a) Measured volumetric strain (b) Measured shear stress

(c) Measured water pressure and outflow (d) Hysteretic stress strain loops

**Figure 7.** Typical time histories measured during cyclic shearing of an unsaturated specimen having an initial suction $\psi_0$ = 10 kPa at the relative density of 0.70

Volumetric strains experienced by the unsaturated specimens fluctuated remarkably in each cycle due to the applied large cyclic strains. Evolutions of the medium volumetric strain in each cycle for all the specimens are shown in Figure 8 for the three relative densities. Matric suction was observed to have a nonnegligible effect at lower relative densities, especially for the specimens at $D_r$ = 0.45 shown in Figure 8(a). The volumetric strains at the end of shearing deviated significantly for different matric suctions with the smallest value of 5.5% at the suction of 10kPa and the larges value of 8.7% at the suction of 4 kPa. For all the relative densities evaluated in this study, higher suction led to a stiffer response in drained conditions and thus less seismic compression, which agrees well with the findings in Kimoto et al. (2011).

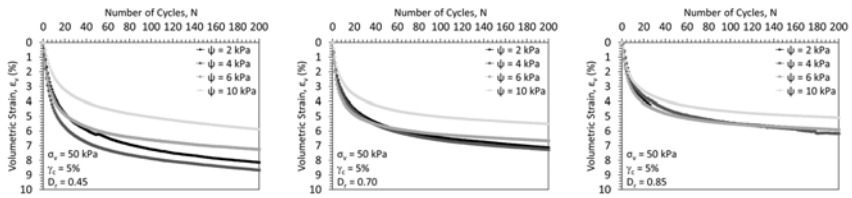


(a) $D_r = 0.45$ (b) $D_r = 0.70$ (c) $D_r = 0.85$

**Figure 8.** Evolution of volumetric strains of unsaturated specimens subjected to $\gamma_c = 5\%$

Volumetric strains for unsaturated specimens at all relative densities at the end of shearing (N = 200) were plotted against matric suction in Figure 9. It can be seen that higher relative density resulted in smaller volumetric contractions for the same suction level, however, this effect is weakened with increased suctions, especially at the highest suction of 10 kPa. At each relative density, suction plays an important role on the seismic compression with lower volumetric strain observed for specimens with higher suctions. However, the effect of suction can be alleviated or lessened by increasing the relative density. Evolutions of the SSCC can be inferred from the tracked water outflows and the degree of saturation, shown in Figure 9 as well. Compared with the initial SSCCs in Figure 3(a), suction stress shifted to the right in the higher suction range at the three relative densities with a remarkable shift at $D_r = 0.45$ and slighter changes at $D_r = 0.70$ and $D_r = 0.85$, which were primarily due to the different amount of volumetric contractions at each relative density.

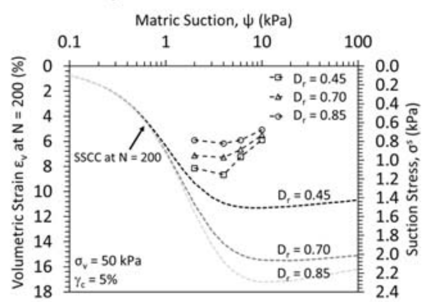


**Figure 9.** Synthesized results with the evolutions of SSCCs at different relative densities

## 8 Conclusion

In this study, a series of strain-controlled cyclic simple shear tests were performed on unsaturated sands with four initial suctions at each of the three relative densities in drained conditions, which represented the worst-case scenario for the near-surface compacted unsaturated backfills in transportation systems. Test results indicated that matric suction could lead to stiffer responses of unsaturated specimens in drained conditions, with the smallest volumetric contraction happened at the highest suction value. However, the dependence of the volumetric response on suction can be alleviated or weakened by increasing relative density. In addition, increasing relative density can remarkably decrease the seismic compression at lower suction values, but not an efficient approach for unsaturated soils in the residual saturation with high suctions.

## References


1. ASTM D6528. Standard Test Method for Consolidated Undrained Direct Simple Shear Testing of Cohesive Soils. ASTM International. West Conshohocken, PA(2017).
2. Bishop, A.W.: The principle of effective stress. Teknisk Ukeblad, 106(39), 859-863(1959).
3. Duku, P.M., Stewart, J.P., Whang, D.H., and Yee, E.: Volumetric strains of clean sands subject to cyclic loads. J. of Geotech. and Geoenv. Eng., 134(8), 1073-1085(2008).
4. Ghayoomi, M., McCartney, J.S., and Ko, H.Y.: Centrifuge test to assess the seismic compression of partially saturated sand layers. Geotechnical Testing Journal, 34(4), 321-331(2011).
5. Hsu, C.C. and Vucetic, M.: Volumetric threshold shear strain for cyclic settlement. J. of Geotech. and Geoenv. Eng., 130(1), 58-70(2004).
6. Kimoto, S., Oka, F., Fukutani, J., Yabuki, T., and Nakashima, K.: Monotonic and cyclic behavior of unsaturated sandy soil under drained and fully undrained conditions. Soils and Foundations, 51(4), 663-681(2011).
7. Lu, N., Godt, J.W., and Wu, D.T.: A closed form equation for effective stress in unsaturated soil. Water Resources Research, 46(5), 55-65(2010).
8. Le, K.N. and Ghayoomi, M.: Cyclic direct simple shear test to measure strain-dependent dynamic properties of unsaturated sand. Geotechnical Testing Journal, 40(3), 381-395(2017).
9. Okamura, M. and Soga, Y.: Effects of pore fluid compressibility on liquefaction resistance of partially saturated sand. Soils and Foundations, 46(5), 695-700(2006).
10. Rong, W. and McCartney, J.S.: Drained seismic compression of unsaturated sand. J. of Geotech. and Geoenv. Eng., 10.1061/(ASCE)GT.1943-5606.0002251(2020).
11. Silver, M.L. and Seed, H.B.: Deformation characteristics of sands under cyclic loading. Journal of Soil Mechanics and Foundations Division, 97(8), 1081-1098(1971).
12. Stewart, J.P., Bray, J.D., McMahon, D.J., Smith, P.M., and Kropp, A.L.: Seismic performance of hillside fills. J. of Geotech. and Geoenv. Eng., 127(11), 905-919(2001).
13. Tokimatsu, K. and Seed, H.B.: Evaluation of settlements in sands due to earthquake shaking. Journal of Geotechnical Engineering, 113(8), 861-878(1987).
14. Unno, T., Kazama, M., Uzuoka, R., and Sento, N.: Liquefaction of unsaturated sand considering the pore air pressure and volume compressibility of the soil particle skeleton. Soils and Foundations, 48(1), 87-99(2008).
15. van Genuchten, M.T.: A closed-form equation for predicting the hydraulic conductivity of unsaturated soils. Soil Science Society of America Journal, 44(5), 892-898(1980).
16. Whang, D.H., Stewart, J.P., and Bray, J.D.: Effect of compaction conditions on the seismic compression of compacted fill soils. Geotechnical Testing Journal, 27(4), 1-9(2004).